Journal of Biomechanics 44 (2011) 2362–2368

Contents lists available at ScienceDirect

Journal of Biomechanics

journal homepage: www.elsevier.com/locate/jbiomech
www.JBiomech.com

Construction of 3D human distal femoral surface models using a 3D statistical deformable model ☆

Zhonglin Zhu [a,b], Guoan Li [a,*]

[a] Bioengineering Laboratory, GRJ-1215, Department of Orthopaedic Surgery, Harvard Medical School/Massachusetts General Hospital, 55 Fruit Street, Boston, MA 02114, USA
[b] Department of Biomedical Engineering, Tsinghua University, Beijing, China

ARTICLE INFO

Article history:
Accepted 4 July 2011

Keywords:
Statistical shape model
Knee
3D knee model
Fluoroscopic images

ABSTRACT

Construction of 3D geometric surface models of human knee joint is always a challenge in biomedical engineering. This study introduced an improved statistical shape model (SSM) method that only uses 2D images of a joint to predict the 3D joint surface model. The SSM was constructed using 40 distal femur models of human knees. In this paper, a series validation and parametric analysis suggested that more than 25 distal femur models are needed to construct the SSM; each distal femur should be described using at least 3000 nodes in space; and two 2D fluoroscopic images taken in 45° directions should be used for the 3D surface shape prediction. Using this SSM method, ten independent distal femurs from 10 independent living subjects were predicted using their 2D plane fluoroscopic images. The predicted models were compared to their native 3D distal femur models constructed using their 3D MR images. The results demonstrated that using two fluoroscopic images of the knee, the overall difference between the predicted distal femur surface and the MR image-based surface was 0.16 ± 1.16 mm. These data indicated that the SSM method could be a powerful method for construction of 3D surface geometries of the distal femur.

1. Introduction

Three-dimensional (3D) surface models of the knee have been extensively utilized in orthopedic surgery and biomechanics research (Barratt et al., 2008; DeFrate et al., 2004; Kobayashi et al., 2009). These included the application in navigation surgeries (Delp et al., 1998), patient-specific implantation and cutting tool designs in knee arthroplasty (Fitz, 2009), as well as in-vivo knee joint motion analysis using the imaging technique (Anderst et al., 2009; DeFrate et al., 2004). In these applications, the joint is usually scanned using CT or MR imaging to acquire a set of 3D images of the joint. The images are then segmented either manually (DeFrate et al., 2004) or automatically (Fripp et al., 2006; Heinze et al., 2002) to construct 3D joint models. In general, construction of the 3D knee joint model is not a trivial procedure. CT imaging needs to expose the subject to radiation and the soft tissue structures are usually not observable. It is difficult to automatically segment MR images and it is always a time-consuming procedure using manual segmentation. A convenient, accurate method for construction of 3D knee joint model is yet to be developed.

Recently, statistical shape model (SSM) method has been established as a useful tool for reconstruction of patient-specific 3D surface models of bony structures, such as the hip or proximal femur using a single radiographic image of the joint (Zheng and Schumann, 2009a; Zheng et al., 2007), or using bi-planar images (Lamecker et al., 2004; Tang and Ellis, 2005; Zheng and Schumann, 2009b), or multi-plane images (Sadowsky et al., 2007; Tang and Ellis, 2005; Zheng et al., 2009c). In this method, a joint database is constructed first using a group of joint shapes to extract the characteristic factors of their surface geometry and construct a deformable training joint shape model. Using the SSM and plane images of a target joint, the training joint model can deform through an optimization procedure until its projection outlines on the image planes of the target joint can match that of the target joint so as to re-create the surface shape model of the target joint (Heimann and Meinzer, 2009). There are few studies that have reconstructed patient-specific 3D models of the knee joint with an accuracy around 1 mm (Barratt et al., 2008; Laporte et al., 2003; Tang and Ellis, 2005). The feasibility and accuracy of this method for construction of 3D human knee joint has not been well defined.

Therefore, in this paper, we propose to utilize the 2D knee joint fluoroscopic images to predict the 3D human distal femur shape using an improved SSM method. The SSM database was constructed first using the femurs of normal subjects. Surface models of 10 independent femurs of normal subjects were then

☆ All authors have made substantial contributions to this manuscript.

* Corresponding author. Tel.: +1 617 726 6472; fax: +1 617 724 4392.
E-mail address: gli1@partners.org (G. Li).

0021-9290/$ - see front matter © 2011 Elsevier Ltd. All rights reserved.
doi:10.1016/j.jbiomech.2011.07.006

constructed using the SSM method. The predicted distal femur models were compared to the native 3D femur models constructed using their 3D MR images. The objective is to examine the feasibility and accuracy of using 2D fluoroscopic images to predict 3D surface shape models of the human distal femur.

2. Material and methods

2.1. Statistical shape model (SSM) of human distal femurs

Forty normal adults were recruited for construction of the SSM of the distal femur with IRB approved. The demographic data of this group subjects is shown in Table 1. One knee of each subject was MR image scanned in sagittal plane using a 3-T MR scanner (MAGNETOM Trio, Siemens, Malvern, PA) and a double-echo water excitation sequence with a surface coil. The MR scans generated sagittal plane images of the knee (512×512 pixels) with a field view of 16 cm $\times$ 16 cm and slice thickness of 1 mm. The MR images of each knee was input into a solid modeling program (Rhinoceros®, Robert McNeel & Associates, Seattle, WA) for construction of a 3D knee joint model (Li et al., 2008). After the bony contour of the knee joint was manually digitized from the MR images, additional points along the bony surface were created using 3D Spatial Interpolation method implemented in MATLAB2010a® software in the transverse planes with 1 mm increments so that the surfaces of all joints in the SSM can be consistently described. A typical procedure to create a mesh model of the distal femur that was constructed from MR images is shown in Fig. 1.

An average distal femur model was constructed using the 40 knees in the SSM. The models of all knee joints were automatically aligned by the method of the iterative closest points (Besl and McKay, 1992). This method determines the best possible alignment between two models by minimizing the distance between their surfaces. A cubic bounding box was used to decide a local coordinate system of the femur (Fig. 2). The posterior tangent joining the medial and lateral condyles in the transverse view was horizontal; meanwhile each femur's distal tangent was horizontal in the coronal view. We use the method of building 3D point pair to calculate the average shape after aligning all models (Zheng et al., 2006). Due to the complicated femoral geometry, each femur model was separated into 3 portions (Fig. 1). A half sphere was fitted into each portion of the femur. The location of the sphere was in the geometric center of the cubic bounding box of the portion. The paired points of all bone models at each portion were found by vectors from the center of sphere to fixed points on the spherical surface. Each vector passed though a femoral surface and found several points on the surface that were close to the vector. One intersection was calculated by the vector and a curved surface fitted using these points. The number of points to present each femur model was therefore the same using the template sphere method. Meanwhile, the intersections along any one radial direction were grouped as paired, corresponding points.

Table 1
The demographic data of the 40 subjects used to construct the SSM.

Subjects	**Sex (male/female)**	**Age (Yrs)**	**Weight (lbs)**	**Height (in.)**	**Femur (right/left)**
Avg	24M/16F	29.9	171.7	69.5	22R/18L
Std		9.7	32.0	3.2	

After all the surface points (x_i,y_i,z_i) were paired, the shape information of all knees was acquired and was used as a learning sample set (S_i), which is also called point distribution model in literature (Zheng et al., 2006). To build a SSM, the method of principal component analysis (PCA) was used to find the variation in the positions of the paired points of the subject (Cootes et al., 1995) through a covariance matrix. The sample set (S_i) was used to build a covariance matrix (Cov)

$$\begin{cases} Cov = \frac{1}{p-1}\sum_{i=1}^{p}(S_i-\bar{S})(S_i-\bar{S})^T \text{ with } S_i=(x_1,y_1,z_1 \ldots x_n,y_n,z_n)^T, \bar{S}=\frac{1}{p}\sum_{i=1}^{p}S_i, \quad i=1:p, \end{cases} \tag{1}$$

where p is the number of knees in the sample set and n is the nodal number of each model. The eigen values and eigen vectors of the Cov are then calculated

$$\begin{cases} \text{eigen value} = (\lambda_1,\lambda_2,\ldots\lambda_s), \lambda_1 \geq \lambda_2 \ldots \geq \lambda_s \geq 0 \\ \text{eigen vector} = (P_1,P_2,\ldots P_s) \end{cases}. \tag{2}$$

The PCA for distal femur models captures geometric features of the models using the eigen values and eigen vectors. The first principal component stands for the largest variation depending on the direction and location of all models. Using the eigen-analysis, a new SSM surface S' can be obtained (Cootes et al., 1995)

$$\begin{cases} S' = M\bar{S} + M\sum_{j=1}^{s} f(\lambda_j)P_j \\ f(\lambda_j) = a_j\sqrt{\lambda_j} \\ M = \frac{1}{p}\sum_{i=1}^{p} M_i \end{cases}, \tag{3}$$

where P_j is an eigen vector and the dimension of P_j is $1 \times (3n)$, a_j is a vector of weights that is used to generate a new shape model (SSM) and M_i is a transformation matrix that transforms the ith knee model in the SSM from its local coordinate system to the global coordinate system.

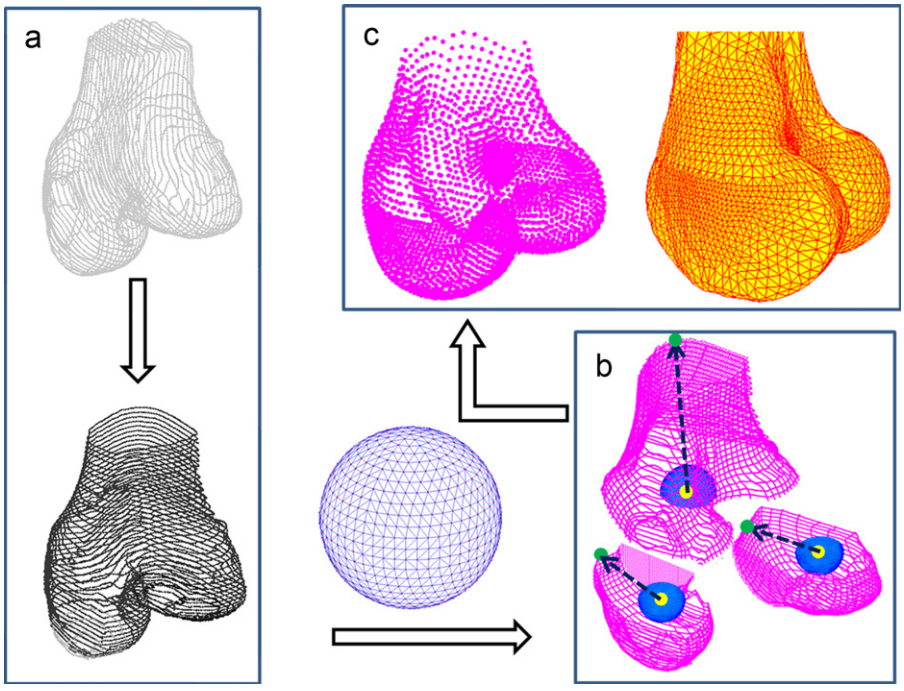

Fig. 1. Each femur model was interpolated with more points in the transverse plane (a) and separated into 3 portions (b) to find the points (c) on the surface along the radial direction of the template sphere.

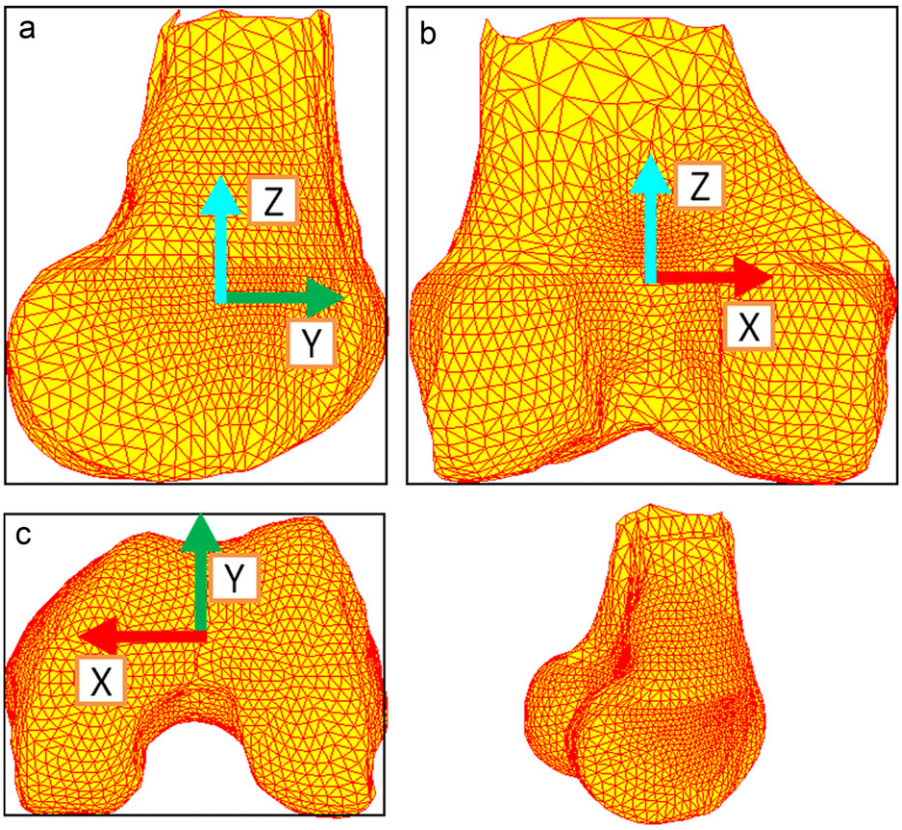

Fig. 2. A typical distal femur model of one subject's left knee in the sagittal (a), coronal (b) and transverse (c) views.

2.2. 2D/3D reconstruction

A SSM surface S' can be deformed based on the average model ($\bar{S}$) and an additional deformation information ($f(\lambda_j)$) (see Eq. (3)). Before predicting the surface shape of a specific joint, an important step is to determine the initial position of the average model in space. To decide the vector of weights a_j using the outline information of the joint on its 2D projected images, a 2D–3D registration procedure is used, which is similar to the 2D–3D image automatic matching procedure that was described previously (Bingham and Li, 2006).

To do this, a knee is imaged using a dual fluoroscopic system. The dual fluoroscopic images are input into the solid software Rhinoceros to construct a virtual fluoroscopic system (Bingham and Li, 2006). Since there is no 3D femoral model corresponding to the actual femur in the fluoroscopic images, it is difficult to define the accurate position of the average model in space. To estimate this position, each model S_i of the SSM training set is projected in the virtual fluoroscopic system to find a position M_i (Bingham and Li, 2006). In this paper, all positions of the models are decided using the dual fluoroscopic techniques. The average of all the optimized positions, M, is defined as a position to place the average model. The SSM surface model S' was then placed in the virtual system and is projected onto the virtual image intensifier (Fig. 3). An objective function (F) is established to minimize the distance between the outline (L_1) of the SSM surface S' and the outline (L_2) of the actual joint projection on the image intensifier (Fig. 3) as described in Bingham and Li (2006)

$$F = \min_{\{a_j\}}(|L_1 - L_2|), \tag{4}$$

where $\{a_j\}$ are optimization variables. If more than one 2D fluoroscopic image is used for the model prediction, the above optimization procedure is then formulated as

$$F = \min_{\{a_j\}}\left(\sum_{k=1}^{n}|L_1^k - L_2^k|\right), \tag{5}$$

where n is the number of 2D images and k represents the kth 2D image. At each step of the optimization, the set of weights (a_i) will be used to obtain a new SSM surface S' through Eq. (3). Therefore, the converged 3D SSM surface S' can be used to represent the actual knee joint model.

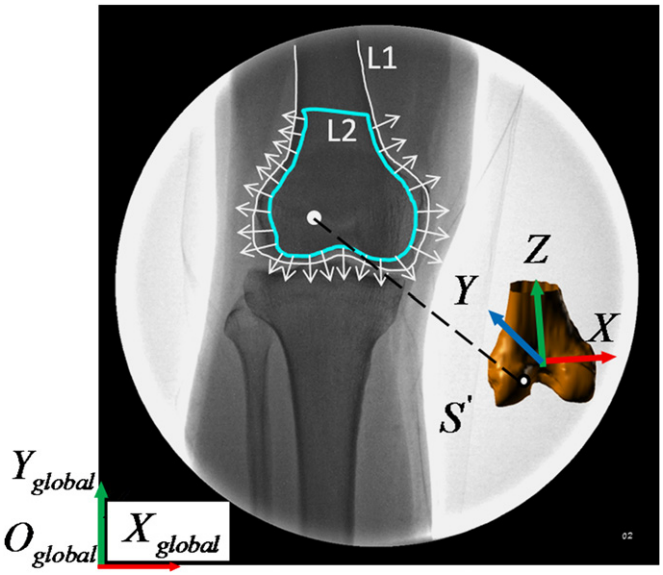

Fig. 3. Projection of the SSM model on the fluoroscopic image intensifier and the deformation of the model when compared to the projection of the actual joint.

2.3. Accuracy validation

The predicted SSM surface S' through the optimization procedure was compared to the corresponding native 3D knee joint model constructed using its 3D MR images, which was considered as the ground truth in this paper. In order to calculate the differences between the predicted model and the MRI model (termed as error in this paper), the SSM was re-meshed and set the distance between any two neighboring nodes as 1 mm. The closest distance from each node of the re-meshed model to the surface of the MRI model was calculated as the surface error. The points outside of MRI model were defined as positive error and inside were

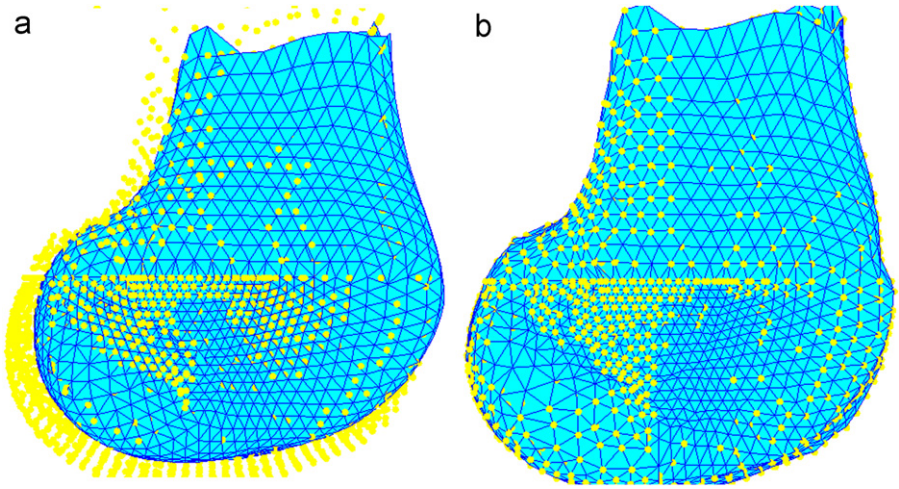

Fig. 4. Process of deformation by the SSMs: (a) to automatically locate the SSM and deformation by minimizing the distance between the outline of the SSM model projection and the outline of the actual joint on the fluoroscopic image. Yellow points are the ground truth MRI model; (b) after the SSM deformation, the SSM is expanded or shrinked to predict the target joint model. (For interpretation of the references to color in this figure legend, the reader is referred to the web version of this article.)

negative (Fig. 4). The average (Avg) errors, standard deviation (Std), the maximum (Max) errors, and the average of the absolute values of the errors (ABS Avg) were reported. In order to present the distribution of all errors of each predicted model, we also reported the histogram of error distribution along the predicted surfaces. Finally, the validation was done by analyzing the overall average errors of the 10 independent living subjects.

2.3.1. Effect of the nodal points of SSMs

When using the SSM method to predict the joint surface, there are several parameters in the algorithms that have to be determined first. We first determined the effect of the nodal numbers that are used to describe each femoral model. An independent target mesh model as a ground truth was projected on the virtual fluoroscopic intensifier to get the virtual 2D fluoroscopic images. The ground truth model was projected at every 10° from 0 (lateral view) to 180° (medial view) when rotated along the long axis of the femur. The reconstruction of this model was then processed by the SSM method. The test included a single image test using the 19 images one by one and a dual image test from any two orthogonal images of the 19 images.

To examine the effect of nodal numbers of the SSM models, the distal femur models in the SSM were described using 1000–10,000 nodes with 1000 increment. The above tests were performed using each definition of the nodal numbers in the SSM models. We analyzed and compared the overall error from the tests to determine how many points would be needed to describe a SSM.

2.3.2. Effect of the model number in the SSM

The prediction of a surface model may be affected by the number of surface models used to construct the SSM training model. No study has examined the effect of the number of models in the SSM on the predicted surfaces. In this paper, various numbers of SSM sample set from 10 to 40 with 5 increment were investigated independently to reconstruct a new model. The error of the surface model predicted using either single or dual images as a function of the model number in the SSM was analyzed using an independent distal femur.

2.3.3. The effect of the number of images in 2D/3D reconstruction

An independent subject femur model was used to test the appropriate number of 2D images for prediction of the femur surfaces. The subject was imaged at every 10° from 0 (lateral view) to 180° (medial view) when rotated along the long axis of the femur. We tested using one single image up to 19 images set up for prediction of the distal femur surface of the subject.

2.3.4. Prediction of distal femur surfaces of subjects

In this paper, we tested the feasibility and accuracy of the SSM technique using 10 independent 3D knee joint models under IRB guidance. After establishing the SSM method, we constructed 10 independent human distal femur models (Table 2). These subjects were fluoroscopically imaged from 2 directions (~45° anterior-medially and anterior-laterally). The 2D images were used to construct the distal femur surface models using the optimization procedure described in Eq. (5). To validate the surface models, the knees of the subjects were imaged using 3D MR scanner in a similar way as done for the above 40 subjects of the SSM. The surface models were similarly constructed using the Rhinoceros software (Li et al., 2008).

Table 2
The demographic data of the 10 subjects recruited to predict their distal femurs using the SSM.

Subjects	**Sex (male/female)**	**Age (Yrs)**	**Weight (lbs)**	**Height (in.)**	**BMI (kg/m^2)**	**Femur (right/left)**
Avg	5M/5F	38.3	171.9	68.6	25.73	5R/5L
StD		8.9	19.3	3.3	2.1	

All optimizations were performed using a PC (Intel(R) Core(TM) i7 processor: 2.67 GHz, 9 GB RAM) on the MATLAB platform. The average time for predicting a femur surface was provided.

3. Results

Using different nodal numbers to describe the femur surface models in the SSM, the average error and standard deviation of the predicted surface were shown in Table 3, where the femoral surfaces were predicted using both one and two 2D images. The model of 3000 nodes has similar average error and standard deviation compared to those models having more nodes. Therefore, we selected 3000 nodes for all the following calculations.

Using different numbers of knee models in the SSM to construct the distal femur model, the average error and standard deviation of the predicted distal femur were shown in Table 4. The prediction is affected by the number of surface models in the SSM. If 10 models are used in the SSM, the accuracy of the predicted model is -0.30 ± 1.28 mm in the single plane test and -0.13 ± 0.88 mm in the dual planes test. When the number of models is above 25, the predicted surface modes are similar.

Different numbers of 2D images were used to predict the distal femoral surface model of one subject (Table 5). Using a single image, the average accuracy of the predicted model is 0.27 ± 1.1 mm and the average of the absolute error (ABS Avg) is 0.84 mm. The accuracy obtained using two 2D images was -0.03 ± 0.61 mm and the average of the absolute error is 0.46 mm, which was similar to those obtained using more than two images. Therefore, two 2D images were used to predict the distal femur of the 10 subjects in this paper.

Table 3
The average error and standard deviation of the predicted distal femur models using different nodal numbers in the SSM.

Accuracy (mm)	Using single image						Using dual images					
Points	Avg	Std	Max	Min	ABS Avg	Time (s)	Avg	Std	Max	Min	ABS Avg	Time (s)
1000	0.08	0.96	2.96	−2.80	0.72	15	0.03	0.66	2.00	−1.95	0.50	32
2000	0.10	0.91	2.83	−2.64	0.69	20	0.03	0.66	2.00	−1.95	0.49	44
3000	0.10	0.96	2.97	−2.77	0.73	25	0.03	0.64	1.95	−1.90	0.48	58
4000	0.06	0.93	2.84	−2.73	0.71	34	0.02	0.65	1.98	−1.94	0.50	71
5000	0.09	0.90	2.80	−2.63	0.69	39	0.05	0.65	1.98	−1.89	0.49	89
6000	0.09	0.91	2.81	−2.63	0.69	46	0.05	0.63	1.95	−1.85	0.48	105
7000	0.10	0.92	2.85	−2.65	0.70	54	0.05	0.64	1.96	−1.86	0.49	118
8000	0.07	0.91	2.79	−2.66	0.70	61	0.01	0.64	1.93	−1.90	0.48	130
9000	0.07	0.92	2.82	−2.68	0.70	84	0.05	0.63	1.95	−1.85	0.48	174
10,000	0.06	0.93	2.84	−2.72	0.70	97	0.02	0.65	1.96	−1.92	0.49	200

Table 4
The average error and standard deviation of the predicted distal femur using different sample numbers in the SSM.

Accuracy (mm)	Using single image						Using dual images					
SSM sample set	Avg	Std	Max	Min	ABS Avg	Time (s)	Avg	Std	Max	Min	ABS Avg	Time (s)
10	−0.30	1.28	3.53	−4.14	0.94	8	−0.13	0.88	2.50	−2.76	0.69	13
15	−0.20	1.08	3.04	−3.45	0.80	12	−0.14	0.85	2.40	−2.68	0.68	19
20	−0.18	1.09	3.10	−3.46	0.81	20	−0.12	0.86	2.46	−2.69	0.69	31
25	−0.13	1.04	2.98	−3.24	0.78	22	−0.14	0.87	2.47	−2.74	0.67	55
30	−0.19	1.06	2.98	−3.36	0.80	29	−0.10	0.81	2.34	−2.54	0.65	53
35	−0.17	1.02	2.89	−3.22	0.77	34	−0.06	0.77	2.27	−2.38	0.60	47
40	−0.17	1.00	2.82	−3.15	0.75	34	0.00	0.78	2.32	−2.33	0.60	74

Table 5
The average error and standard deviation of the predicted distal femur using different numbers of 2D fluoroscopic images.

Images	Accuracy (mm)					Time (s)
	Avg	Std	Max	Min	ABS Avg	
1	0.27	1.10	3.58	−3.04	0.84	108
2	−0.03	0.61	1.81	−1.87	0.46	101
3	−0.04	0.52	1.52	−1.61	0.39	194
4	0.01	0.67	2.02	−2.01	0.50	189
5	0.01	0.45	1.35	−1.34	0.33	364
6	0.06	0.47	1.48	−1.36	0.37	399
7	0.02	0.43	1.30	−1.26	0.31	343
8	0.00	0.36	1.07	−1.08	0.27	382
9	0.07	0.42	1.33	−1.19	0.32	521
10	0.01	0.45	1.35	−1.33	0.33	430
11	0.03	0.44	1.36	−1.29	0.34	440
12	0.04	0.37	1.14	−1.06	0.28	520
13	0.05	0.40	1.25	−1.14	0.30	656
14	0.06	0.39	1.24	−1.11	0.30	856
15	0.03	0.39	1.19	−1.14	0.30	817
16	0.03	0.44	1.35	−1.29	0.34	757
17	0.07	0.38	1.22	−1.08	0.30	1025
18	0.08	0.40	1.28	−1.13	0.31	1087
19	0.06	0.39	1.22	−1.10	0.30	1196

The error distribution of one typical subject was shown in the Fig. 5. It is in a Gaussian distribution with a mean error of 0.2 mm and standard deviation of 0.66 mm. In all these 10 femurs, the average errors between the MRI model and the predicted distal femur using the SSM model were less than 1.0 mm and standard deviation within 1.5 mm (Table 6). Using a weighted mean method, the overall average error of the 10 knees was 0.16 mm and standard deviation is 1.16 mm. The overall average of the absolute error is 0.90 mm. The average computation time of all femur models was 178 s.

4. Discussion

Construction of 3D bony surface models of the human knee joint is an important step for many navigation surgeries and image-based in-vivo knee kinematics studies (Anderst et al., 2009; DeFrate et al., 2004; Delp et al., 1998). Although, CT and MR image scanning techniques have been widely used, it is always a time-consuming and technically challenging problem in biomedical engineering. This study introduced a numeric technique to predict the 3D surface models of human distal femurs. The average differences between the predicted surface shapes and the surface shapes constructed from MR images of 10 human distal femurs was less than 0.2 mm.

Prediction of bony surface models has been extensively investigated in literature (Buchaillard et al., 2007; Luthi et al., 2009; Rajamani et al., 2007; Sadowsky et al., 2007; Styner et al., 2003). In prediction of human vertebral shapes, Zheng et al. (2010) used one lateral fluoroscopic image to predict the vertebral shape with the mean reconstruction error between 0.7 and 1.6 mm and the standard deviation between 0.6 and 1.4 mm in a validation using cadaveric bones. In application to human pelvic, Sadowsky et al. (2007) predict the surface shape with an accuracy between 1.42 and 2.17 mm and maximum error between 7.73 and 12.37 mm in the leave-one-out test. Few studies have also predicted the distal femoral end shape (Fleute et al., 1999; Laporte et al., 2003; Tang and Ellis, 2005). Laporte et al. (2003) utilized two orthogonal images of the knee and a SSM constructed using 8 CT knee models to reconstruct the target femur shape with an accuracy of 1.0 mm and RMS 1.3 mm. Compared with the published data, our results showed improved accuracy on the surface shape prediction of human distal femur (0.16 ± 1.16 mm).

The prediction of the distal femur surface is affected by the number of surface models used to construct the SSM training model. In literature, various numbers of models have been used to construct the SSMs. For example, Schumann et al. (2010) used 30 proximal femoral CT models; Tang and Ellis (2005) used 20 femoral CT models;

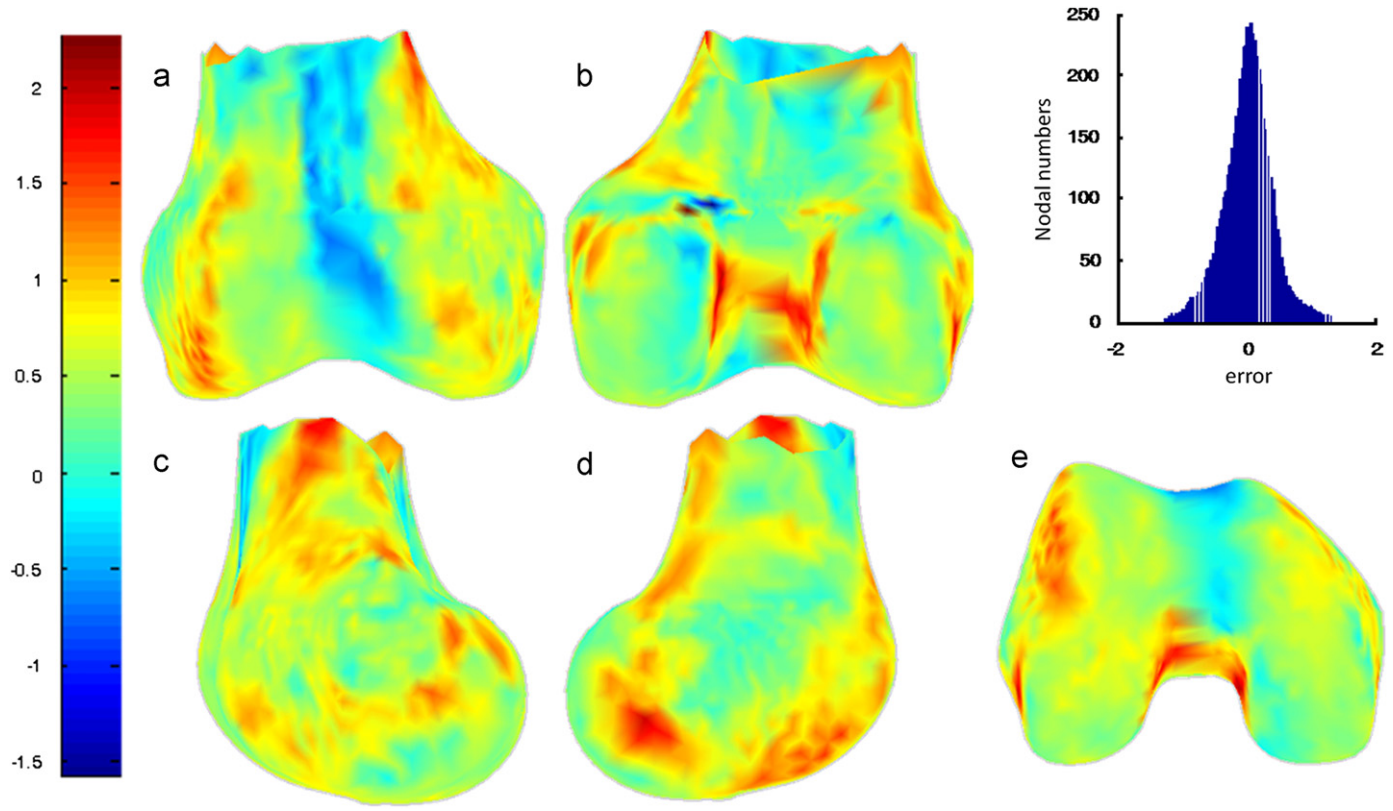

Fig. 5. Error distribution of a typical right femur (No. 3) in the anterior (a), posterior (b), medial (c), lateral (d) and axial (e) view.

Table 6
The error and standard deviation of the distal femoral surface models of the 10 subjects predicted using two 2D fluoroscopic images and the SSM.

Subjects	Accuracy (mm)					Time (s)
	Avg	Std	Max	Min	ABS Avg	
1	0.82	1.53	5.41	−3.77	1.28	218
2	−0.10	1.30	3.80	−3.99	0.98	164
3	0.20	0.66	2.17	−1.77	0.54	126
4	0.55	1.47	4.97	−3.86	1.22	200
5	0.06	1.26	3.84	−3.72	0.85	131
6	−0.14	1.18	3.40	−3.68	0.88	299
7	0.06	0.95	2.90	−2.78	0.71	154
8	−0.35	1.14	3.08	−3.78	0.90	141
9	0.17	0.96	3.05	−2.71	0.72	238
10	0.30	1.10	3.61	−3.01	0.89	108
Weighted mean	0.16	1.16	3.62	−3.31	0.90	178

Buchaillard et al. (2007) used 22 teeth micro-CT models; Sadowsky et al. (2007) used 110 pelvis CT models to construct the SSM. We used 40 MR image-based human femur models to construct the SSM in this paper. Theoretically, more the models in the SSM, more complete the geometric features to be captured in the SSM of the joint. Our data indicated that when the number of models is above 25, the predicted surface modes are similar.

We predicted the joint surfaces using ordinary fluoroscopic images. Osseous outlines on the 2D fluoroscopic images are used as guidelines for joint shape prediction through an optimization procedure. No specific landmarks on the joint are necessary. Therefore, the application of this method is rather simple. Although, various numbers of 2D images have been used in literature, our data indicated that using two 2D fluoroscopic images can provide similar accuracy on the surface models when compared to those using more than 2 images. However, the validation of the surface prediction was done by comparing the predicted surface model to that constructed from MR images of the joint since a gold standard joint surface model is not available for living subjects. Therefore, the data should be explained as the differences between the predicted surface and the MR image-based surface, not as an absolute accuracy of the method.

Fluoroscopic images were used for optimization to predict the distal femur shape in this study. A limitation that should be noted is that this method can only be used to predict joint surface model. It cannot predict the 3D bony density model such as those used by You et al. (2001). The human knee models in the SSM were obtained through manual segmentation of the MR images of the knee. In future, a database using CT image models should be established. Different radiographic techniques, such as X-rays, should be evaluated to examine the effect of 2D image modalities on the predicted surface knee joint shape. Another limitation is that there are not enough models to build the SSM based on gender differences. There were previous studies that found the differences between the male and female distal femurs (Mahfouz et al., 2007; Yue et al., 2010). In this paper we are aimed to reconstruct general distal femoral models and evaluate the corresponding errors.

In summary, this study applied an improved SSM method and 2D fluoroscopic images to predict the 3D surface shape models of the knee. The overall average accuracy of the method is within 0.2 mm when 2 fluoroscopic images are used. This method does not require 3D CT or MR imaging of the target joint, thus does not need to involve the image segmentation, which is always a challenge in biomedical engineering. Therefore, the SSM method could be a useful tool for construction of a subject knee joint model using 2D fluoroscopic images. Future studies should extend this method to other bony surfaces such as the tibia, patella.

Conflict of interest statement

The authors of this manuscript have nothing to disclose that would bias our work.

Acknowledgments

This study was partially supported by a grant from National Institutes of Health (R01 AR055612) and a grant from the China Scholarship Council (2010621146)

References

Anderst, W., Zauel, R., Bishop, J., Demps, E., Tashman, S., 2009. Validation of three-dimensional model-based tibio-femoral tracking during running. Medical Engineering and Physics 31, 10–16.

Barratt, D.C., Chan, C.S., Edwards, P.J., Penney, G.P., Slomczykowski, M., Carter, T.J., Hawkes, D.J., 2008. Instantiation and registration of statistical shape models of the femur and pelvis using 3D ultrasound imaging. Medical Image Analysis 12, 358–374.

Besl, P.J., McKay, N.D., 1992. A method for registration of 3-D shapes. IEEE Transactions on Pattern Analysis and Machine Intelligence, 239–256.

Bingham, J., Li, G., 2006. An optimized image matching method for determining in-vivo TKA kinematics with a dual-orthogonal fluoroscopic imaging system. Journal of Biomechanical Engineering 128, 588.

Buchaillard, S.I., Ong, S.H., Payan, Y., Foong, K., 2007. 3D statistical models for tooth surface reconstruction. Computers in Biology and Medicine 37, 1461–1471.

Cootes, T.F., Taylor, C.J., Cooper, D.H., Graham, J., 1995. Active shape models-their training and application. Computer Vision and Image Understanding 61, 38–59.

DeFrate, L.E., Sun, H., Gill, T.J., Rubash, H.E., Li, G., 2004. In vivo tibiofemoral contact analysis using 3D MRI-based knee models. Journal of Biomechanics 37, 1499–1504.

Delp, S.L., Stulberg, S.D., Davies, B., Picard, F., Leitner, F., 1998. Computer assisted knee replacement. Clinical Orthopaedics and Related Research, 49–56.

Fitz, W., 2009. Unicompartmental knee arthroplasty with use of novel patient-specific resurfacing implants and personalized jigs. The Journal of Bone and Joint Surgery (American Volume) 91 (Suppl. 1), 69–76.

Fleute, M., Lavallee, S., Julliard, R., 1999. Incorporating a statistically based shape model into a system for computer-assisted anterior cruciate ligament surgery. Medical Image Analysis 3, 209–222.

Fripp, J., Warfield, S.K., Crozier, S., Ourselin, S., 2006. Automatic segmentation of the knee bones using 3D active shape models. Pattern Recognition 1, 171–174.

Heimann, T., Meinzer, H.P., 2009. Statistical shape models for 3D medical image segmentation: a review. Medical Image Analysis 13, 543–563.

Heinze, P., Meister, D., Kober, R., Raczkowsky, J., Worn, H., 2002. Atlas-based segmentation of pathological knee joints. Studies in Health Technology and Informatics 85, 198–203.

Kobayashi, K., Sakamoto, M., Tanabe, Y., Ariumi, A., Sato, T., Omori, G., Koga, Y., 2009. Automated image registration for assessing three-dimensional alignment of entire lower extremity and implant position using bi-plane radiography. Journal of Biomechanics 42, 2818–2822.

Lamecker, H., Seebass, M., Hege, H.C., Deuflhard, P., 2004. A 3d statistical shape model of the pelvic bone for segmentation. Citeseer, 1341.

Laporte, S., Skalli, W., de Guise, J.A., Lavaste, F., Mitton, D., 2003. A biplanar reconstruction method based on 2D and 3D contours: application to the distal femur. Computer Methods in Biomechanics and Biomedical Engineering 6, 1–6.

Li, G., Van de Velde, S.K., Bingham, J.T., 2008. Validation of a non-invasive fluoroscopic imaging technique for the measurement of dynamic knee joint motion. Journal of Biomechanics 41, 1616–1622.

Luthi, M., Albrecht, T., Vetter, T., 2009. Building shape models from lousy data. Medical Image Computing and Computer Assisted Intervention 12, 1–8.

Mahfouz, M.R., Merkl, B.C., Fatah, E.E.A., Booth, R., Argenson, J.N., 2007. Automatic methods for characterization of sexual dimorphism of adult femora: distal femur. Computer Methods in Biomechanics and Biomedical Engineering 10, 447–456.

Rajamani, K.T., Styner, M.A., Talib, H., Zheng, G., Nolte, L.P., Gonzalez Ballester, M.A., 2007. Statistical deformable bone models for robust 3D surface extrapolation from sparse data. Medical Image Analysis 11, 99–109.

Sadowsky, O., Chintalapani, G., Taylor, R.H., 2007. Deformable 2D–3D registration of the pelvis with a limited field of view, using shape statistics. Medical Image Computing and Computer Assisted Intervention 10, 519–526.

Schumann, S., Tannast, M., Nolte, L.P., Zheng, G., 2010. Validation of statistical shape model based reconstruction of the proximal femur—a morphology study. Medical Engineering and Physics 32, 638–644.

Styner, M.A., Rajamani, K.T., Nolte, L.P., Zsemlye, G., Szekely, G., Taylor, C.J., Davies, R.H., 2003. Evaluation of 3D correspondence methods for model building. Information Processing in Medical Imaging 18, 63–75.

Tang, T.S., Ellis, R.E., 2005. 2D/3D deformable registration using a hybrid atlas. Medical Image Computing and Computer Assisted Intervention 8, 223–230.

You, B.M., Siy, P., Anderst, W., Tashman, S., 2001. In vivo measurement of 3-D skeletal kinematics from sequences of biplane radiographs: application to knee kinematics. IEEE Transactions on Medical Imaging 20, 514–525.

Yue, B., Varadarajan, K.M., Ai, S., Tang, T., Rubash, H.E., Li, G., 2010. Gender differences in the knees of Chinese population. Knee Surgery, Sports Traumatology, Arthroscopy 19, 80–88.

Zheng, G., Schumann, S., 2009a. A system for 3-D reconstruction of a patient-specific surface model from calibrated X-ray images. Studies in Health Technology and Informatics 142, 453–458.

Zheng, G., Schumann, S., 2009b. 3D reconstruction of a patient-specific surface model of the proximal femur from calibrated X-ray radiographs: a validation study. Medical Physics 36, 1155–1166.

Zheng, G., Nolte, L.P., Ferguson, S.J., 2010. Scaled, patient-specific 3D vertebral model reconstruction based on 2D lateral fluoroscopy. International Journal of Computer Assisted Radiology and Surgery (online).

Zheng, G., Ballester, M.A., Styner, M., Nolte, L.P., 2006. Reconstruction of patient-specific 3D bone surface from 2D calibrated fluoroscopic images and point distribution model. Medical Image Computing and Computer Assisted Intervention 9, 25–32.

Zheng, G., Gollmer, S., Schumann, S., Dong, X., Feilkas, T., Gonzalez Ballester, M.A., 2009c. A 2D/3D correspondence building method for reconstruction of a patient-specific 3D bone surface model using point distribution models and calibrated X-ray images. Medical Image Analysis 13, 883–899.

Zheng, G., Dong, X., Rajamani, K.T., Zhang, X., Styner, M., Thoranaghatte, R.U., Nolte, L.P., Ballester, M.A., 2007. Accurate and robust reconstruction of a surface model of the proximal femur from sparse-point data and a dense-point distribution model for surgical navigation. IEEE Transactions on Biomedical Engineering 54, 2109–2122.